OsteoArthritis and Cartilage (2007) **15,** 673–681

doi:10.1016/j.joca.2006.12.010

Osteoarthritis and Cartilage

International Cartilage Repair Society

OARSI OSTEOARTHRITIS RESEARCH SOCIETY INTERNATIONAL

Positron emission tomography with ^{18}F-FDG in osteoarthritic knee

H. Nakamura M.D., Ph.D.†‡*, K. Masuko M.D., Ph.D.‡, K. Yudoh M.D., Ph.D.‡, T. Kato M.D., Ph.D.‡, K. Nishioka M.D., Ph.D.‡, T. Sugihara M.D., Ph.D.§ and M. Beppu M.D., Ph.D.§

† *Department of Joint Disease and Rheumatism, Nippon Medical School, Tokyo, Japan*

‡ *Institute of Medical Science, St. Marianna University, Kawasaki, Japan*

§ *Department of Orthopedics, St. Marianna University, Kawasaki, Japan*

Summary

Objectives: To evaluate osteoarthritis (OA) of the knee using positron emission tomography (PET) with 2-^{18}F-fluoro-2-deoxy-D-glucose (^{18}F-FDG) as a tracer.

Materials and methods: Fifteen patients with medial-type knee OA and three healthy subjects were enrolled in the study. After clinical examination and conventional radiography, ^{18}F-FDG PET and magnetic resonance imaging (MRI) were performed. ^{18}F-FDG uptake was quantified as a standardized uptake value (SUV) and the localization of ^{18}F-FDG uptake was identified using fusion images created with MRI scans.

Results: ^{18}F-FDG generally accumulated in periarticular lesions and was absent in the articular cartilage. SUVs of the whole knee were higher in OA than in controls, and those in the medial condyle were higher than in the lateral condyle in OA. Prominent ^{18}F-FDG uptake was found in the intercondylar notch in OA and extended along the posterior cruciate ligament (PCL) in some cases. Periosteophytic accumulation was found in one-half of cases with definite osteophytes. Accumulation was also found in subchondral lesions and bone marrow, which corresponded with bone edema diagnosed by MRI. No significant correlation was found between SUV and clinical manifestations.

Conclusions: ^{18}F-FDG uptake was upregulated in OA and generally accumulated in periarticular lesions. Increased uptake was found in the intercondylar notch extending along the PCL, periosteophytic lesions, and bone marrow. These results provide *in vivo* pathognomonic insights into OA.

Key words: Osteoarthritis, Knee, PET, MRI.

Introduction

Osteoarthritis (OA) is characterized by degradation and loss of articular cartilage, and remodeling of underlying bone. Currently, conventional radiography is the standard method for diagnosis and evaluation of severity of OA. A standing anteroposterior (AP) view is commonly used to assess articular degradation expressed as joint space width[1,2]; however, this provides only indirect assessment of the articular cartilage, and it takes a couple of years to detect cartilage loss with technical concerns[3–5]. Thus, refined imaging techniques and modalities have been studied to detect molecular properties and metabolic changes in cartilage[4].

*Address correspondence and reprint requests to: Hiroshi Nakamura M.D., Ph.D., Department of Joint Disease and Rheumatism, Nippon Medical School, 1-1-5, Sendagi, Bunkyo-ku, Tokyo 113-8603, Japan. Tel: 81-3-3822-2131; Fax: 81-3-3822-2170; E-mail: nakamura@nms.ac.jp

Received 29 June 2006; revision accepted 29 December 2006.

Magnetic resonance imaging (MRI) can delineate articular cartilage and accurately assess cartilage volume and thickness[6,7]. The cartilage volumes computed by three-dimensional (3D) reconstruction of MRI images are comparable to those evaluated by computed tomography (CT) arthrography and those from surgically removed cartilage. Moreover, glycosaminoglycan (GAG) can be visualized using contrast agents. Gadolinium-diethylenetriamine pentaacetic acid (DTPA) can penetrate into cartilage and distributes inversely with the GAG concentration. Delayed gadolinium-enhanced MRI of cartilage has been validated in clinical and basic scientific studies[8].

Positron emission tomography (PET) demonstrates metabolic changes in target tissues. PET using 2-^{18}F-fluoro-2-deoxy-D-glucose (^{18}F-FDG) reflects glucose metabolism, and can detect the foci of malignant tumors, infection and inflammation[9,10]. ^{18}F-FDG PET is now widely used in oncology[9]; however, its application in rheumatic disease is limited. Synovial volume evaluated by MRI was correlated with the uptake of ^{18}F-FDG in 10 cases of

inflammatory joint disease (two rheumatoid arthritis (RA) and eight other inflammatory arthritis)[11]. Twenty-one patients with RA were evaluated by ^{18}F-FDG PET, and the number of PET-positive joints and the cumulative standardized uptake value (SUV) were significantly correlated with swollen and tender joint counts[12]. Case reports of synovitis, acne, pustulosis, hyperostosis, osteitis (SAPHO) syndrome[13], psoriatic arthritis[14], and RA[15,16] have been published in which ^{18}F-FDG PET was of diagnostic value.

While conventional radiographs and MRI provide morphological information about articular cartilage, PET reflects the glucose metabolism of target organs and provides functional images. As the cartilage matrix is composed of glucosaminoglycan and maintained by the glucose metabolism of chondrocytes, changes in cartilage metabolism might be detected by PET. Although PET is expected to delineate the changes in OA, there have been few reports of ^{18}F-FDG PET in OA. The aim of this study was to evaluate knee OA using ^{18}F-FDG PET images and to obtain preliminary PET features of knee OA.

Patients and methods

PATIENTS

The inclusion criteria included medial-type knee OA fulfilling ACR criteria[17], with any radiological grading in our outpatient clinic. Patients with hyperglycemia were excluded. Fifteen patients were recruited in the study (13 females, two males; average age of 71.5 years). After clinical examination (effusion, swelling, rest pain, motion pain, and tenderness), the patients underwent AP view radiography in the standing position to evaluate the Kellgren/Lawrence (K/L) grade[18]. About 1 week later, they were subjected to MRI and ^{18}F-FDG PET on the same day. Young, healthy volunteers (one female, two males; average age of 26.3 years) were also investigated. The study was approved by the ethical committee of the institutes.

MRI

To identify the site of ^{18}F-FDG accumulation, MRI was undertaken. Before PET examination, MRI was performed on a Gyroscan Intera 1.5 T (Philips, Netherlands) with a microscopy coil (47 mm). Coronal images were acquired with a proton density-weighted sequence (repetition time = 1500 ms, echo time = 15 ms, thickness = 2 mm, field of vision = 8 cm) and a fat-suppressed sequence (repetition time = 20 ms, echo time = 9.8 ms, flip angle = 30°, thickness = 2 mm, field of vision = 8 cm). The patients lay supine, and the leg was set with a specific triangular pillow to obtain an identical position in the PET examination. For fusion images, both MRI and PET scans started at exactly 5 cm proximal to the upper end of the patella.

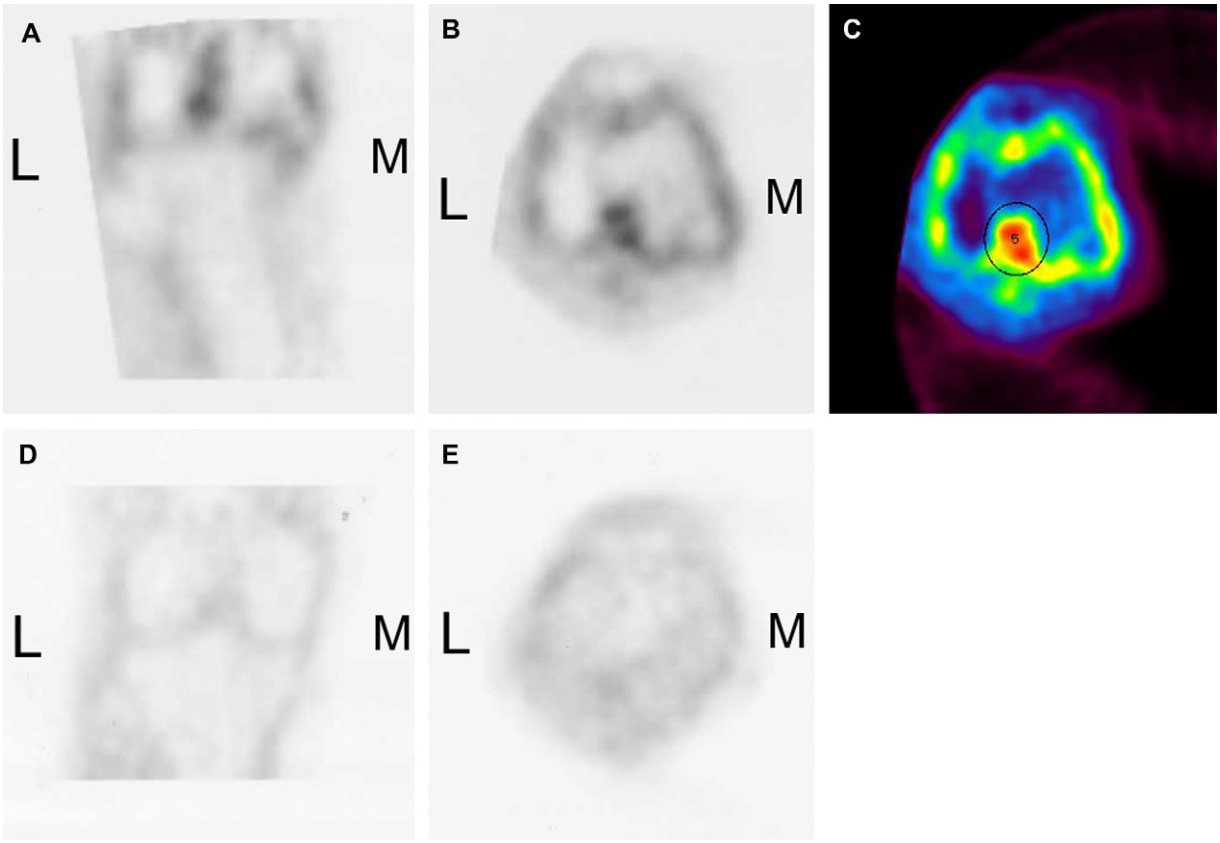

Fig. 1. Representative coronal (A,D) and axial (B,C,E) sections of PET images in a knee with OA (A–C) and in a control knee (D,E). ^{18}F-FDG uptake was emphasized by sequential colorization ranging from red (high) to blue (low) (C). ^{18}F-FDG commonly accumulated in the periarticular region and was lacking in the articular cartilage. M: medial, L: lateral.

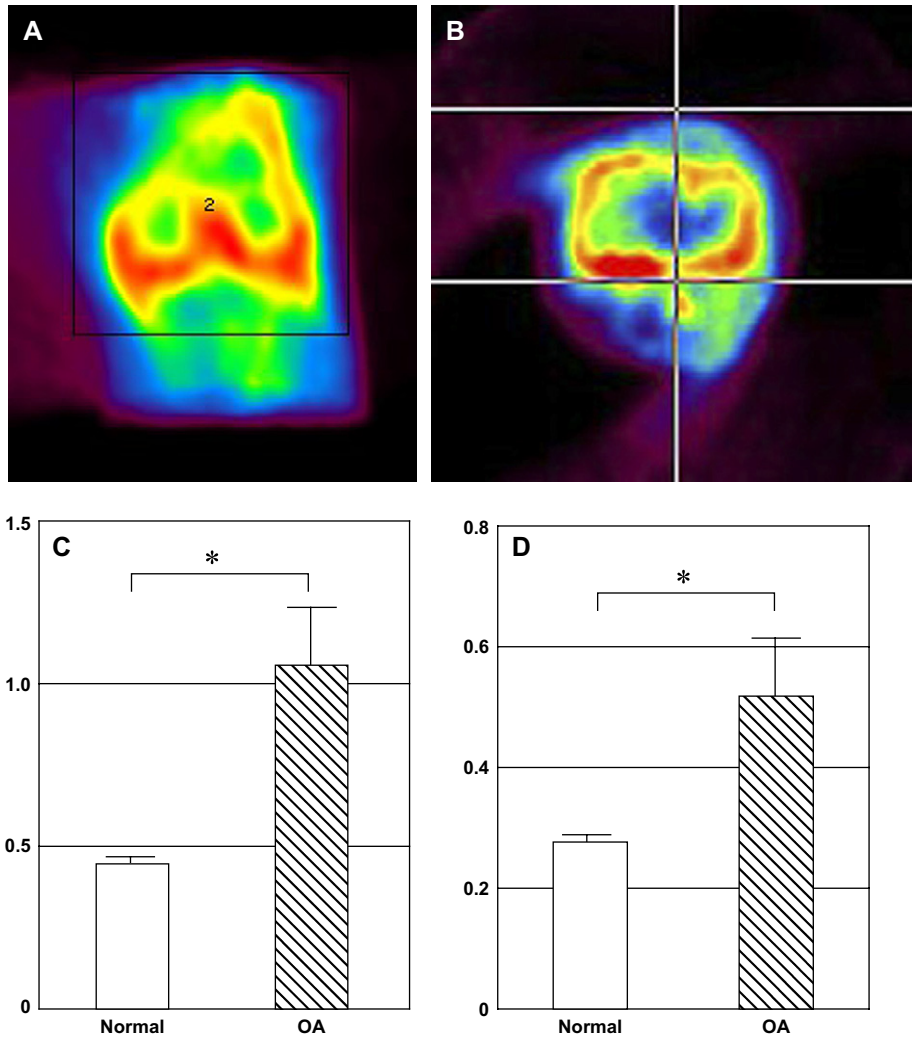

Fig. 2. The SUVs of whole knees were assessed using 3D data (A,B). Both peak (C) and mean (D) SUVs were significantly higher in OA than in controls. The data were expressed as the mean and standard deviation, and compared using Student's *t*-test. $^{*}P < 0.01$.

^{18}F-FDG PET

^{18}F-FDG PET was performed using an Eminence SET-3000G (Shimazu, Japan) operated in 3D mode. The effective field of view was 256 mm in the *x*-, *y*-, and *z*-directions. The patients fasted for at least 6 h before injection and were at rest for 15 min after injection to reduce muscular uptake. Before injection, blood glucose levels were measured; in all cases, they were under 100 mg/dL. The patients were injected with ^{18}F-FDG (3.5 MBq/kg) in a peripheral vein, with imaging 50 min after the injection. This optimal interval was determined by a time-course study performed in advance. Semiquantitative ^{18}F-FDG uptake was expressed as the SUV normalized for the lean body mass.

DIGITAL IMAGE PROCESSING

Digital images were processed using a high-performance graphic system (Virtual Place; AZE, Japan). To assess SUV, the region of interest was positioned arbitrarily on a 3D image, values were calculated, and an SUV was determined for each knee. SUV intensity was colored to emphasize the uptake intensity ranging from red (high) to blue (low) as needed. Digital data were transferred to the system and fusion images were created automatically with some manual adjustment. To observe the localization of ^{18}F-FDG closely, the fusion images focused on the medial compartment.

STATISTICAL ANALYSIS

SUVs in OA and healthy controls were compared using Student's *t*-test, and the medial and lateral condyles were compared with a paired *t*-test. The relationship of SUVs with clinical manifestations and radiological grading was analyzed by Student's *t*-test and one-way analysis of variance (ANOVA), respectively.

Results

^{18}F-FDG UPTAKE IN KNEE OA AND SUV

Figure 1 shows representative coronal and axial sections of PET images in a knee with OA [Fig. 1(A)–(C)] and in

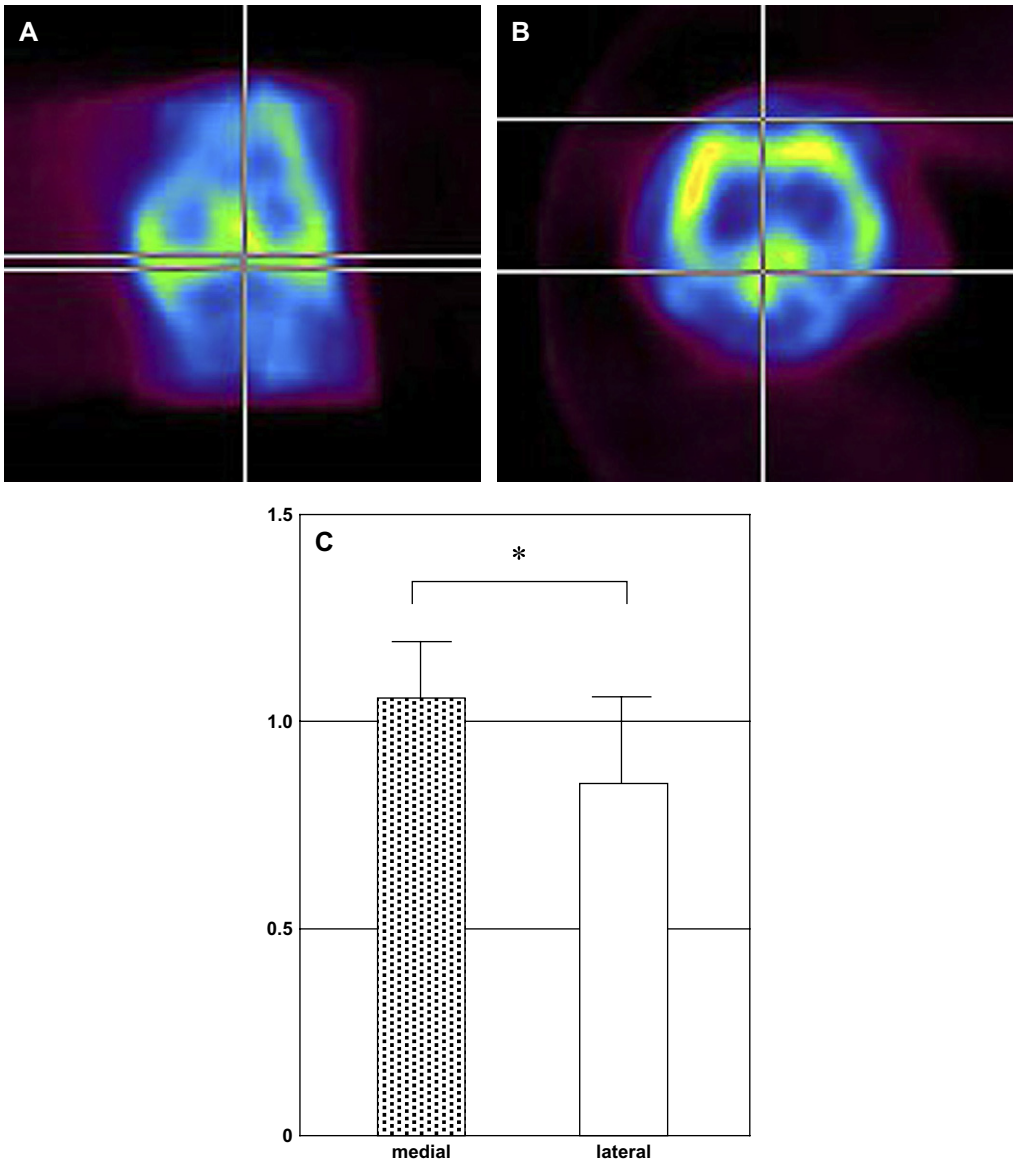

Fig. 3. SUVs at the joint level were compared between the medial condyle and the lateral condyle (A,B). SUVs of the medial condyle were higher than those of the lateral condyle (C). The data were expressed as the mean and standard deviation, and compared using a paired *t*-test. $^{*}P < 0.05$.

a control knee [Fig. 1(D) and (E)]. ^{18}F-FDG commonly accumulated in the periarticular region and was lacking in the articular cartilage. While the knee joint was demarcated by various signal intensities in OA, there was little uptake of ^{18}F-FDG in the controls. Accumulation of ^{18}F-FDG in the intercondylar notch was a prominent feature in knee OA [Fig. 1(C)]. A high uptake in the intercondylar lesion was seen in 13 of 15 knees, and the mean SUV in the lesion was 1.085 ± 0.21, whereas that of the whole knee joint was 0.519 ± 0.10.

The SUVs of whole knees were assessed using 3D data [Fig. 2(A) and (B)]. Both mean and peak SUVs were significantly higher in OA than in controls [Fig. 2(C) and (D)]. When the SUVs were compared between the medial condyle and the lateral condyle at the joint level, the former levels were significantly higher than the latter (Fig. 3).

LOCALIZATION OF ^{18}F-FDG ACCUMULATION IN INDIVIDUAL CASES

Serial fusion images of MRI and PET were made to specify the location of ^{18}F-FDG accumulation. Twelve knees had definite osteophytes and six of these (50%) showed high accumulation of ^{18}F-FDG around the osteophytes (Fig. 4). High accumulation of ^{18}F-FDG in the intercondylar notch was observed in most cases, and the accumulation extended along the posterior cruciate ligament (PCL) in four knees (Fig. 5, Table I). ^{18}F-FDG accumulation was found in the subchondral region of the medial tibial condyle in four cases. Enhanced uptake was limited in the subchondral lesion of the base of the osteophytes in three knees. The lesions gave a low signal on proton density-weighted MRI and a high signal on fat-suppressed MRI, suggesting bone edema (Fig. 6).

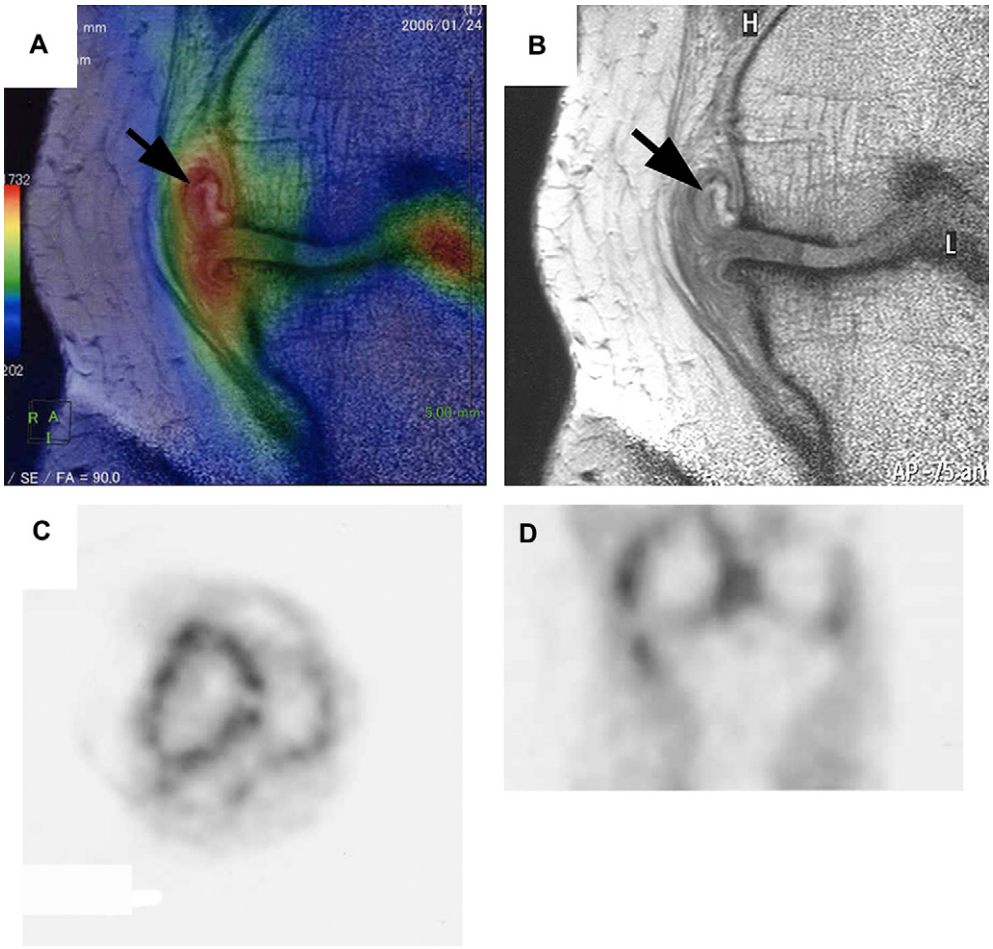

Fig. 4. ^{18}F-FDG accumulation was found around medial osteophyte (Arrow). (A) Fusion image, (B) MRI, (C) PET axial view, and (D) PET coronal view.

In another case, extensive ^{18}F-FDG uptake was found in the bone marrow, spreading out into the medial soft tissue that was speculated to be synovium or ligament (Fig. 7).

PET FINDINGS AND CLINICAL MANIFESTATIONS

Maximum SUV and mean SUV were compared between patients with and without clinical findings: effusion, swelling, and rest pain; however, no significant difference was observed between them. Similarly, SUVs were compared between radiological grading and no significant relation was found (Table II).

Discussion

PET images can delineate the distribution of inflammatory tissue such as synovitis. Although OA has inflammatory aspects[19], PET has received little attention in OA till date. As far as we know, there is only one report evaluating shoulder OA by ^{18}F-FDG PET[20]. In this report, the ^{18}F-FDG uptake pattern of shoulder OA was circumferential and diffused, and they speculated that this finding reflected the presence of mild synovitis. In our series, a periarticular pattern was a common finding in knee OA, and the SUVs in OA were significantly higher than those in young, healthy controls. Thus, higher SUVs in knee OA also suggested the presence of synovitis.

Apart from peripheral uptake, high ^{18}F-FDG accumulation was found in the intercondylar notch with various intensities in OA, and the accumulation extended along the PCL in some cases. It has been reported that ligament damage is more common in painful knee OA[21]. Thus, ligament tear may be one of the causes of ^{18}F-FDG accumulation around the PCL, as well as periligamentous synovitis. In addition, accumulation of ^{18}F-FDG was found around osteophytes. Osteophytes represent new bone formation associated with cartilaginous differentiation similar to fetal growth plate cartilage[22]. In these regions, metabolism is upregulated in terms of GAG production and new bone formation. Enhanced ^{18}F-FDG uptake around osteophytes reflects the upregulated metabolism of osteochondral tissue in osteophytes and/or soft tissue inflammation around osteophytes.

^{18}F-FDG accumulation was found in bone marrow lesions. These lesions gave a low signal on proton density-weighted MRI and a high signal on fat-suppressed MRI. Similar bone marrow changes in knee OA have been reported as bone edema[23], and these lesions

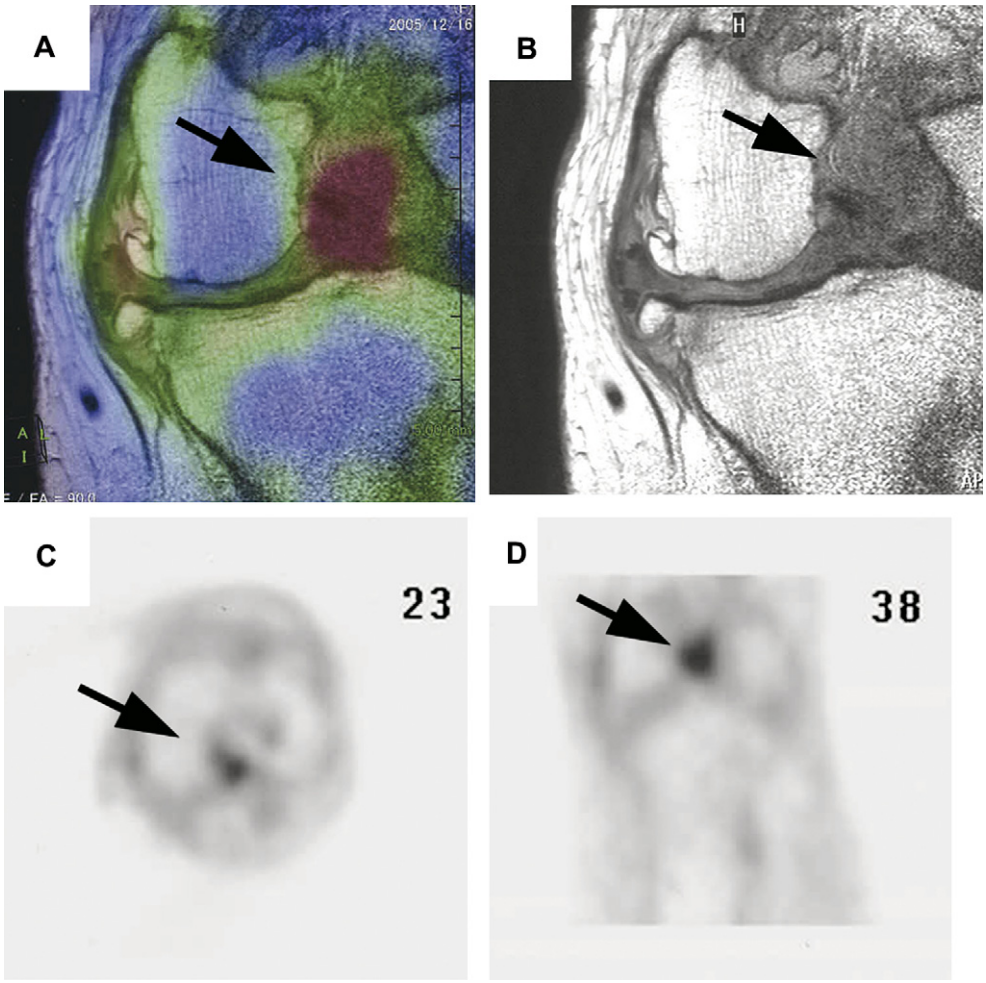

Fig. 5. ^{18}F-FDG accumulation extended along PCL (Arrow). (A) Fusion image, (B) MRI, (C) PET axial view, and (D) PET coronal view.

were correlated with malalignment of the lower extremities and predicted focal deterioration. Histologically, these lesions show abnormal bone with excessive fibrosis, small areas of osteonecrosis, and extensive bony remodeling[24]. Thus, a change in OA is not restricted to the cartilage and synovium, but also occurs in bone marrow. Moreover, bone edema might be influenced by circumferential inflammation. As matrix production is enhanced in the earlier stages of OA[25], ^{18}F-FDG uptake is expected to be high. However, no enhanced uptake was found in articular cartilage, even in the lower K/L grade knees.

The limitations of our study include the lack of an adequate number of age-matched comparisons. As this was a preliminary study of ^{18}F-FDG PET in knee OA, contrastive subjects were selected as controls. As far as we know, no age-related changes in PET of joints have been elucidated. To validate the diagnostic value of PET, early-stage OA should be also assessed.

In summary, ^{18}F-FDG uptake was upregulated in OA, commonly accumulating in periarticular regions. Interestingly, increased uptake was seen in the intercondylar notch and accumulation was found along the PCL. ^{18}F-FDG uptake was also found in bone marrow lesions. These results provide *in vivo* pathognomonic insights into OA.

Table I
Demographic features and ^{18}F-FDG uptake

Case	Age	Sex		K/L	SUV		Accumulation pattern	
					Maximum	Mean	peri PCL	Subchondral region
1	51	F	R	1	0.70	0.36	+	
2	51	F	R	3	1.06	0.42	+	+
3	58	F	R	3	0.96	0.45		
4	68	F	L	3	0.90	0.42		+
5	68	F	L	4	1.33	0.68		
6	72	F	L	3	1.12	0.58		
7	73	F	R	1	1.09	0.56		
8	75	F	L	3	1.08	0.58	+	+
9	76	F	L	1	1.57	0.64		+
10	76	F	R	2	0.93	0.47		
11	78	F	L	3	1.05	0.56		
12	79	M	L	2	1.39	0.70		
13	80	F	L	2	0.80	0.40		
14	81	M	R	3	0.90	0.44	+	
15	87	F	R	4	1.10	0.54		

R: Right, L: Left, +: Present.

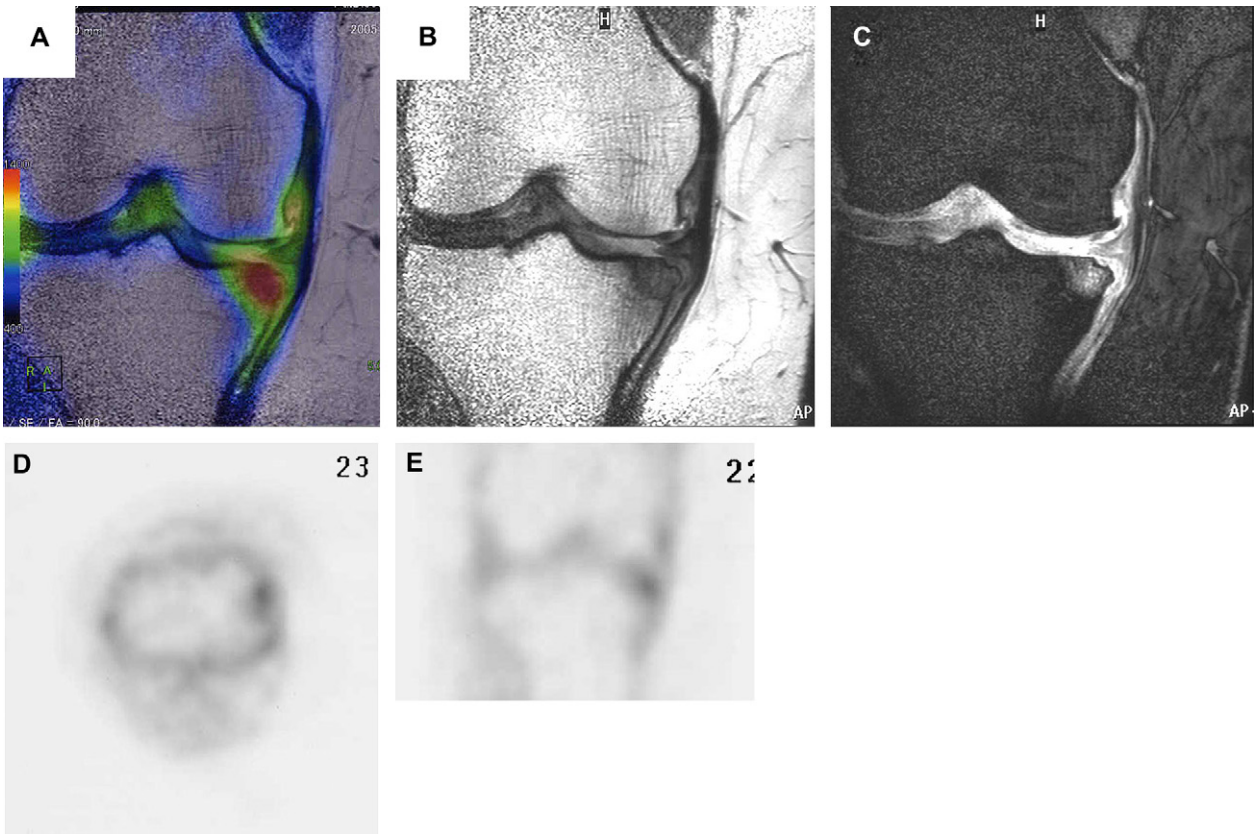

Fig. 6. ^{18}F-FDG accumulated in the subchondral lesion of the base of the osteophytes. MRI study suggested the lesion as bone edema. (A) Fusion image, (B) proton density-weighted MRI, (C) fat-suppressed MRI, (D) PET axial view, and (E) PET coronal view.

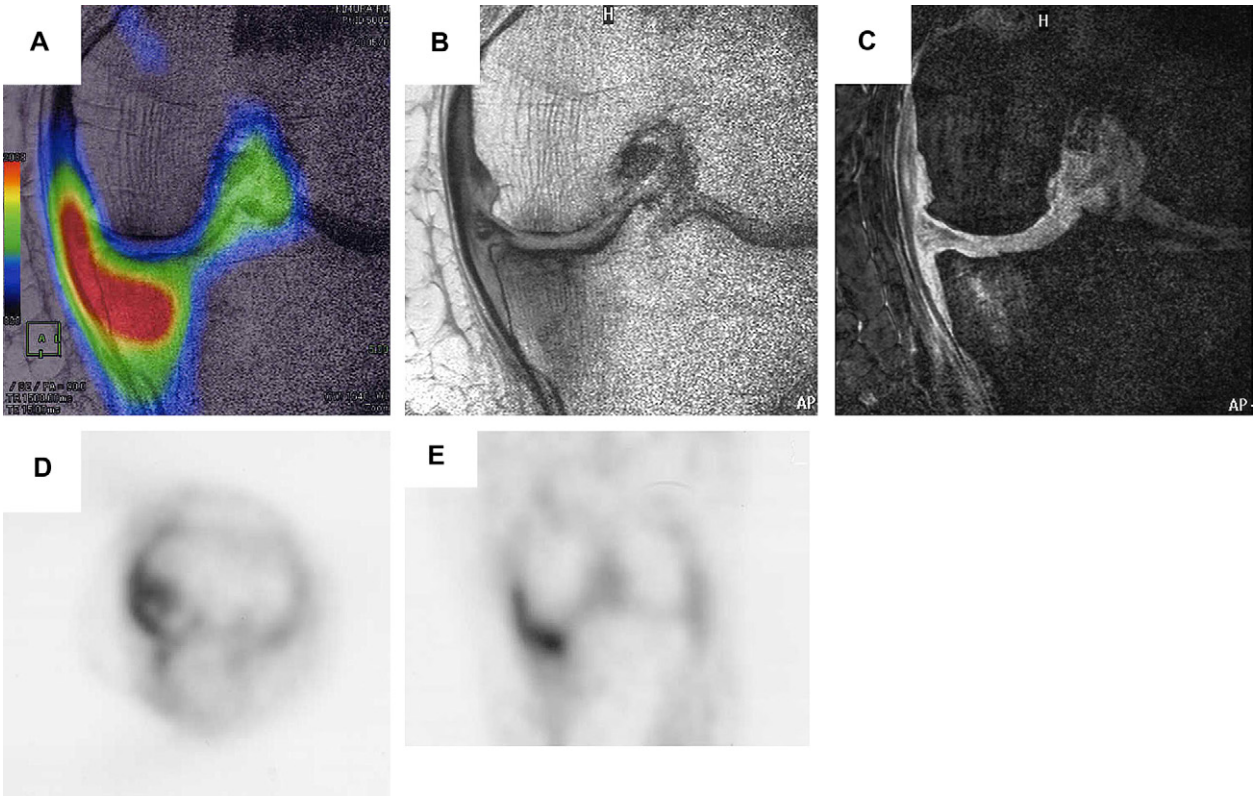

Fig. 7. ^{18}F-FDG uptake was found in the bone marrow, spreading out into the medial soft tissue that was speculated to be synovium or ligament. (A) Fusion image, (B) proton density-weighted MRI, (C) fat-suppressed MRI, (D) PET axial view, and (E) PET coronal view.

Table II
^{18}F-FDG uptake and clinical findings and radiological grading

Clinical findings	Max SUV					Mean SUV				
	Absent	Present			*P*	Absent	Present			*P*
Effusion	1.03 ± 0.17	1.11 ± 0.26			NS	0.50 ± 0.10	0.54 ± 0.10			NS
Swelling	0.89 ± 0.19	1.09 ± 0.21			NS	0.47 ± 0.11	0.53 ± 0.10			NS
Rest pain	1.07 ± 0.25	1.06 ± 0.70			NS	0.50 ± 0.11	0.54 ± 0.09			NS
Radiological grading*	I	II	III	IV		I	II	III	IV	
	1.12 ± 0.36	1.04 ± 0.25	1.01 ± 0.08	1.22 ± 0.44	NS	0.52 ± 0.12	0.52 ± 0.13	0.49 ± 0.07	0.61 ± 0.21	NS

Values were the mean ± SD. Comparisons were made by Student's *t*-test in clinical findings and one-way ANOVA in radiological grading. NS = not significant. * K/L grade.

Acknowledgment

This study was funded by the Ministry of Education, Culture, Sports, Science and Technology of Japan. The authors would like to thank Dr Yukihiko Ozawa and Yoichiro Tasaki and the staff of Yuai Clinic for their imaging and technical support for PET and MRI.

References

1. Reginster JY, Deroisy R, Rovati LC, Lee RL, Lejeune E, Bruyere O, *et al*. Long-term effects of glucosamine sulphate on osteoarthritis progression: a randomised, placebo-controlled clinical trial. Lancet 2001;357: 251–6.
2. Raynauld JP, Buckland-Wright C, Ward R, Choquette D, Haraoui B, Martel-Pelletier J, *et al*. Safety and efficacy of long-term intraarticular steroid injections in osteoarthritis of the knee: a randomized, double-blind, placebo-controlled trial. Arthritis Rheum 2003;48:370–7.
3. Mazzuca SA, Brandt KD. Is knee radiography useful for studying the efficacy of a disease-modifying osteoarthritis drug in humans? Rheum Dis Clin North Am 2003;29:819–30.
4. Buckland-Wright. Radiographic assessment of osteoarthritis: comparison between existing methodologies. Osteoarthritis Cartilage 1999;7:430–3.
5. Mazzuca SA, Brandt KD, Buckwalter KA, Lequesne M. Pitfalls in the accurate measurement of joint space narrowing in semiflexed, anteroposterior radiographic imaging of the knee. Arthritis Rheum 2004;50: 2508–15.
6. Eckstein F, Schnier M, Haubner M, Priebsch J, Glaser C, Englmeier KH, *et al*. Accuracy of cartilage volume and thickness measurements with magnetic resonance imaging. Clin Orthop 1998;352:137–48.
7. Burgkart R, Glaser C, Hyhlik-Durr A, Englmeier KH, Reiser M, Eckstein F. Magnetic resonance imaging-based assessment of cartilage loss in severe osteoarthritis: accuracy, precision, and diagnostic value. Arthritis Rheum 2001;44:2072–7.
8. Gray ML, Eckstein F, Peterfy C, Dahlberg L, Kim YJ, Sorensen AG. Toward imaging biomarkers for osteoarthritis. Clin Orthop 2004;427:S175–81.
9. Juweid ME, Cheson BD. Positron-emission tomography and assessment of cancer therapy. N Engl J Med 2006;354:496–507.
10. Rennen HJ, Corstens FH, Oyen WJ, Boerman OC. New concepts in infection/inflammation imaging. Q J Nucl Med 2001;45:167–73.
11. Roivainen A, Parkkola R, Yli-Kerttula T, Lehikoinen P, Viljanen T, Mottonen T, *et al*. Use of positron emission tomography with methyl-11C-choline and 2-18F-fluoro-2-deoxy-D-glucose in comparison with magnetic resonance imaging for the assessment of inflammatory proliferation of synovium. Arthritis Rheum 2003; 48:3077–84.
12. Beckers C, Ribbens C, Andre B, Marcelis S, Kaye O, Mathy L, *et al*. Assessment of disease activity in rheumatoid arthritis with (18)F-FDG PET. J Nucl Med 2004; 45:956–64.
13. Pichler R, Weiglein K, Schmekal B, Sfetsos K, Maschek W. Bone scintigraphy using Tc-99m DPD and F18-FDG in a patient with SAPHO syndrome. Scand J Rheumatol 2003;32:58–60.
14. Yun M, Kim W, Adam LE, Alnafisi N, Herman C, Alavi A. F-18 FDG uptake in a patient with psoriatic arthritis: imaging correlation with patient symptoms. Clin Nucl Med 2001;26:692–3.
15. Polisson RP, Schoenberg OI, Fischman A, Rubin R, Simon LS, Rosenthal D, *et al*. Use of magnetic resonance imaging and positron emission tomography in the assessment of synovial volume and glucose metabolism in patients with rheumatoid arthritis. Arthritis Rheum 1995;38:819–25.
16. Kaneta T, Hakamatsuka T, Yamada T, Takase K, Sato A, Higano S, *et al*. Atlantoaxial osteoarthritis in rheumatoid arthritis: FDG PET/CT findings. Clin Nucl Med 2006;31:209.
17. Altman R, Asch E, Bloch D, Bole G, Borenstein D, Brandt K, *et al*. Development of criteria for the classification and reporting of osteoarthritis. Classification of osteoarthritis of the knee. Diagnostic and Therapeutic Criteria Committee of the American Rheumatism Association. Arthritis Rheum 1986;29:1039–49.
18. Kellgren JIT, Lawrence JS. Radiographic assessment of osteoarthritis. Ann Rheum Dis 1957;16:499–502.
19. Pelletier JP, Martel-Pelletier J, Abramson SB. Osteoarthritis, an inflammatory disease: potential implication for the selection of new therapeutic targets. Arthritis Rheum 2001;44:1237–47.
20. Wandler E, Kramer EL, Sherman O, Babb J, Scarola J, Rafii M. Diffuse FDG shoulder uptake on PET is associated with clinical findings of osteoarthritis. AJR Am J Roentgenol 2005;185:797–803.
21. Conaghan PG, Felson D, Gold G, Lohmander S, Totterman S, Altman R. MRI and non-cartilaginous structures in knee osteoarthritis. Osteoarthritis Cartilage 2006;14(Suppl 1):87–94.
22. Gelse K, Soder S, Eger W, Diemtar T, Aigner T. Osteophyte development—molecular characterization of differentiation stages. Osteoarthritis Cartilage 2003; 11:141–8.

23. Felson DT, McLaughlin S, Goggins J, LaValley MP, Gale ME, Totterman S, *et al*. Bone marrow edema and its relation to progression of knee osteoarthritis. Ann Intern Med 2003;139:330–6.
24. Bergman AG, Willen HK, Lindstrand AL, Pettersson HT. Osteoarthritis of the knee: correlation of subchondral MR signal abnormalities with histopathologic and radiographic features. Skeletal Radiol 1994;23:445–8.
25. Sandy JD, Adams ME, Billingham ME, Plaas A, Muir H. *In vivo* and *in vitro* stimulation of chondrocyte biosynthetic activity in early experimental osteoarthritis. Arthritis Rheum 1984;27:388–97.